Journal of Medicinal Plants and By-products (2027) 2: 190– 196

Open Access Full Text Article

Bioinformatic Characterization and Molecular Dynamics Simulations of Cliotide U1 Interactions with Model Bacterial Phospholipid Bilayers

Mahnaz Nasre Taheri[1], Mehdi Goudarzi[2]*, Gholamhossein Ebrahimipour[1]* and Ali Hashemi[2]

[1] *Department of Microbiology and Microbial biotechnology, Faculty of life sciences and Biotechnology, Shahid Beheshti University, Evin, Tehran, Iran*
[2] *Department of Microbiology, School of Medicine, Shahid Beheshti University of Medical Sciences, Tehran, Iran*

Article Info

Article Type
Original Article

Article History
Received: 25 February 2026
Accepted: 10 August 2026
© 2012 Iranian Society of Medicinal Plants.
All rights reserved.

***Corresponding authors**

Mehdi Goudarzi
Gholamhossein Ebrahimipour, Department of Microbiology, Faculty of Biological Sciences and Technology, Shahid Beheshti University, Tehran, Iran
m.goudarzi@sbmu.ac.ir

Gholamhossein Ebrahimipour
Department of Microbiology, School of Medicine, Shahid Beheshti University of Medical Sciences, Tehran, Iran
g-ebrahimi@sbu.ac.ir

ABSTRACT

The worldwide rise in multidrug-resistant (MDR) microorganisms has intensified efforts to identify novel antimicrobial strategies beyond traditional antibiotics. This study presents a comprehensive *in silico* bioinformatic and molecular dynamics (MD) analysis of the antimicrobial peptide Cliotide U1, derived from *Urtica dioica*, to elucidate its structural properties, predicted toxicity profile, and membrane interaction mechanisms against Gram-positive and Gram-negative bacteria. In silico toxicity and hemolytic predictions using ToxinPred and HemoPI classified Cliotide U1 as a non-toxic and non-hemolytic peptide, while dPABBs analysis revealed potential anti-biofilm activity. Structural modeling and helical wheel analysis indicated that the peptide adopts a stable amphipathic α-helical structure, with cationic and hydrophobic residues optimally distributed for membrane binding. A 1000-ns all-atom MD simulation of Cliotide U1 in an aqueous environment was conducted to evaluate its structural stability, whereas separate 100-ns MD simulations were performed to investigate peptide interactions with model bacterial phospholipid bilayers using the CHARMM36 force field. In the peptide–membrane simulations, Cliotide U1 showed favorable interactions with the Gram-negative membrane. In contrast, limited surface interaction with Gram-positive membranes was observed, suggesting a carpet-like mechanism of action. RMSD and RMSF analyses indicated higher structural stability and lower fluctuations in the Gram-negative system. Overall, these computational findings identify Cliotide U1 as a predicted stable, selective, and low-toxicity antimicrobial peptide capable of potentially disrupting bacterial membranes through electrostatic and hydrophobic interactions. This peptide holds promise as a natural candidate for the development of next-generation antimicrobial agents, although experimental validation is required to confirm these predictions.

Keywords: Cliotide U1, *Urtica dioica*, Antimicrobial Peptides, Molecular Dynamics Simulation, Anti-Biofilm Activity

How to cite this paper
Nasre Taheri, M., Goudarzi, M., Ebrahimipour, G., Hashemi, A. Bioinformatic Characterization and Molecular Dynamics Simulations of Cliotide U1 Interactions with Model Bacterial Phospholipid Bilayers. Journal of Medicinal Plants and By-products, 2027;16 (2): 190- 196. doi: 10.22034/jmpb.2027.372251.2148

INTRODUCTION

Today, the indiscriminate use of antibiotics has increased drug resistance and has become a global concern [1]. Scientists have focused on replacing antibiotics with safe and natural components that have high antibacterial activity to treat bacterial infections [2-6]. Antimicrobial peptides (AMPs) have emerged as a promising class of therapeutic agents in the fight against multidrug-resistant (MDR) pathogens. Unlike conventional antibiotics, which often target specific metabolic pathways, AMPs act primarily by disrupting microbial membranes, thereby reducing the likelihood of resistance development [7]. These peptides are generally small, cationic, and amphipathic molecules found in a wide range of living organisms. The rise in antibiotic resistance has created an urgent demand for new strategies to combat infectious diseases, and therefore, AMPs have become a major focus in experimental and computational biomedical research [8].

Computational approaches, particularly bioinformatics and molecular dynamics (MD) simulations, have become essential tools for elucidating the structure–function relationships of AMPs. Bioinformatic analyses enable the identification of conserved motifs, prediction of secondary structure, and evaluation of

physicochemical properties such as charge distribution and hydrophobicity [9]. On the other hand, *in silico* molecular dynamics simulations provide atomistic insights into the dynamic interactions between peptides and lipid bilayers, which are critical for understanding the mechanisms of membrane disruption [10]. These simulations are particularly useful for investigating peptide selectivity towards Gram-positive and Gram-negative bacteria, which differ significantly in membrane composition. Gram-positive bacteria have a thick peptidoglycan layer and negatively charged phospholipids, while Gram-negative bacteria have an asymmetric bilayer with lipopolysaccharides (LPS) in the outer layer, which creates further barriers to peptide penetration [11].

Several studies have used molecular modeling and MD simulations to assess the interactions of AMPs with model lipid bilayers. For example, recent *in silico* studies have shown that cationic AMPs preferentially interact with the negatively charged phosphatidylglycerol and cardiolipin lipids, leading to membrane thinning, pore formation, or carpet-like disruption [12, 13].

Furthermore, *in silico* strategies can reduce experimental costs and time by predicting the efficacy and stability of candidate peptides before laboratory validation [13]. By simulating peptide interactions with both Gram-positive and Gram-negative bilayer models, researchers can assess selectivity, penetration depth, and structural stability. Such computational studies can also guide rational modifications of peptide sequences to increase antimicrobial potency while minimizing toxicity toward mammalian membranes [14]. Given the serious global health challenge of antimicrobial resistance, integrating bioinformatics with MD simulation offers a powerful strategy to accelerate the discovery and optimization of novel AMPs.

In our previous study, Cliotide U1 (LIVAASLVYDFYTWI AKKVALLRIAKKVLYLARNA), a novel 35 residues antimicrobial peptide with an α-helical structure, was isolated from *Urtica dioica* leaves and was found to be active against Gram-positive and Gram-negative bacteria without significant cytotoxicity and hemolytic activity [15]. Understanding how Cliotide U1 interacts with bacterial membranes at the molecular level could provide new insights into its antimicrobial mechanism and potential clinical applications. In this study, we performed a comprehensive bioinformatic characterization of Cliotide U1, followed by MD simulations of its interactions with model Gram-positive and Gram-negative bilayer lipids. By combining sequence analysis, structural modeling, and dynamic simulations, we aim to elucidate the physicochemical properties and membrane interaction profiles of Cliotide U1. Findings of the present research are expected to enhance our knowledge of plant-derived peptides as antimicrobial agents and provide a theoretical framework for their further experimental validation and therapeutic development.

MATERIALS AND METHODS

In silico Prediction of Hemolysis, Toxicity, and Antibiofilm Activity

The hemolytic activity of Cliotide U1 was assessed using the HemoPI server (batch mode) (https://webs.iiitd.edu.in/raghava/hemopi/batch.php) [16]. In parallel, potential peptide toxicity was evaluated with ToxinPred (https://webs.iiitd.edu.in/raghava/toxinpred/design.php) [17]. To further explore functional potential relevant to biomedical applications, the antibiofilm activity of Cliotide U1 was estimated through the dPABBs web server (http://ab-openlab.csir.res.in/abp/antibiofilm/peptide.php) [18].

Helical Propensity and Residue Distribution

Because electrostatic attraction between cationic residues and negatively charged bacterial membranes is a key feature of many antimicrobial peptides, and hydrophobic residues contribute to membrane insertion and stabilization [19], the residue distribution and helical parameters of Cliotide U1 were analyzed using HeliQuest (https://heliquest.ipmc.cnrs.fr/index.html) [20].

Molecular Dynamics Simulation of the Peptide in Aqueous Environment

All-atom classical MD simulations were conducted in GROMACS 2023 [21] to examine peptide behavior in an aqueous environment. The peptide topology was generated using the CHARMM36 force field [22]. The peptide was positioned at the center of a cubic box solvated with TIP3P water, maintaining a minimum distance of 1.0 nm from the peptide to each box edge. The system was neutralized and adjusted to physiological ionic strength by adding Na/Cl^- ions to 0.15 M. Energy minimization was performed using the steepest descent algorithm for 5000 steps, followed by equilibration under NVT conditions for 3 ns at 37°C and subsequent NPT equilibration for 5 ns at 1 bar and 37°C. Production MD was then carried out for 1000 ns.

Bond constraints were applied using the LINCS algorithm [23]. Long-range electrostatics were computed with the Particle Mesh Ewald (PME) method, while short-range van der Waals and Coulomb interactions used a 1.2 nm cut-off. Temperature and pressure were controlled with a V-rescale thermostat and a C-rescale barostat, respectively. Trajectories were saved every 1.2 ns for downstream analyses.

Construction and Equilibration of Lipid Bilayers

Representative Gram-positive and Gram-negative lipid bilayers were generated using CHARMM-GUI [24]. Each membrane was composed of phosphatidylglycerol (PG), phosphatidylethanolamine (PE), and cardiolipin (CL) at defined ratios based on previous membrane models [25,26]. As summarized in Table 1, each bilayer contained 78 lipid molecules along with the associated water layers. The CHARMM-GUI protocol was followed, including an initial energy minimization (1000 steps) and six equilibration stages (500 ps each) under controlled temperature and pressure [21]. An additional 5-ns NPT simulation was performed to ensure further relaxation of each bilayer. The area per lipid along the X/Y plane and across the Z-axis was quantified using GridMAT-MD v2.0 [27].

Peptide–membrane MD Simulations

To prepare for membrane-interaction simulations, the Cliotide U1 structure was first energy-minimized and equilibrated at 310 K and 1 atm, followed by a short MD run (20 ns) to relax the peptide. The peptide was then placed approximately 3 nm above the membrane surface using CHARMM-GUI Membrane Builder [24]. The systems were neutralized and supplemented with Na^+/Cl^- ions (system compositions are provided in Table 1).

Table 1 Components of the bilayer and peptide–bilayer system

Membrane	Lipid type			SOD	CLA	Ion concentration	Distance
	PG	PE	CL				
Gram-negative membrane	12	62	4	107	49	15	3 nm
Gram-positive membrane	46	0	32	189	33	24	3 nm

Each peptide–membrane system underwent energy minimization followed by six consecutive NVT equilibration steps (500 ps each) generated by CHARMM-GUI. After transferring the systems into GROMACS, additional minimization and equilibration under NVT and NPT ensembles were performed for 20 ns, after which production simulations were run for 100 ns for each peptide–membrane complex.

Control bilayers (Gram-positive and Gram-negative) without the peptide were prepared and simulated under the same conditions for 100 ns. Simulations were performed under constant temperature and pressure, allowing lateral fluctuations and peptide movement along the membrane plane (NPZT-like behavior). Periodic boundary conditions were applied in all dimensions, enabling unrestricted peptide diffusion in the solvent.

When the peptide center of mass approached the buffer boundary, a conservative repulsive potential was applied to prevent boundary artifacts without imposing external forces within the buffer region. Temperature was maintained at 310 K using a Langevin thermostat, while pressure was controlled semi-isotropically at 1 bar using the Parrinello–Rahman algorithm (tp = 2 ps) [28]. All systems used CHARMM36, and simulations were run in GROMACS 2023.3 [29] with a 2-fs time step. LINCS constrained covalent and hydrogen bonds. A switching distance of 1.0 nm was applied, with short-range electrostatic and van der Waals cut-offs of 1.2 nm. Long-range electrostatics were treated using PME with FFT under periodic boundary conditions.

Data Processing and Visualization

GROMACS internal modules were used to analyze the MD simulations. Numerical processing and figure preparation were carried out using Microsoft Excel and OriginPro (version 2022). The peptide–membrane distance was computed using the lipid phosphorus atoms and the peptide center of mass. Visual inspection and rendering were performed with VMD [30], and video editing was carried out using the Kapwing online platform (https://www.kapwing.com/).

RESULTS AND DISCUSSION

Hemolytic Activity, Toxicity, and Antibiofilm Activity

All analyses in this section were performed using *in silico* prediction tools; no wet-lab assays were conducted in the present study. The present bioinformatic and MD simulation study of the antimicrobial peptide Cliotide U1 from *Urtica dioica* provides valuable insight into the structure–function relationships underlying its selective antibacterial activity.

Table 2 *In silico* evaluation of hemolytic, toxic, and anti-biofilm properties of Cliotide U1

ID	Toxinpred		HemoPI	dPABB	
	Result	SVM score	PROB score	SVM score	Prediction
Cliotide U1	Non-toxic	-1.1	0.49	0.85	Biofilm active

This peptide showed potent activity, especially against Gram-negative bacteria, which can be attributed to its amphipathic α-helical structure, stable folding dynamics, and favorable electrostatic interactions with negatively charged lipid bilayers.

Table 3 Intrachain hydrogen-bonding residues (donor and acceptor sites)

No.	Donor residue	Acceptor residue	No.	Donor residue	Acceptor residue
1	:ALA5:HN	:LEU1:O	26	:LEU21:HN	:LYS17:O
2	:ALA5:HN	:ILE2:O	27	:LEU22:HN	:LYS18:O
3	:SER6:HN	:ILE2:O	28	:LEU22:HN	:VAL19:O
4	:SER6:HG1	:ILE2:O	29	:ARG23:HN	:VAL19:O
5	:LEU7:HN	:VAL3:O	30	:ILE24:HN	:ALA20:O
6	:LEU7:HN	:ALA4:O	31	:ALA25:HN	:LEU21:O
7	:VAL8:HN	:ALA4:O	32	:LYS26:HN	:LEU22:O
8	:TYR9:HN	:ALA5:O	33	:LYS27:HN	:ARG23:O
9	:ASP10:HN	:SER6:O	34	:VAL28:HN	:ILE24:O
10	:PHE11:HN	:LEU7:O	35	:LEU29:HN	:ALA25:O
11	:PHE11:HN	:VAL8:O	36	:LEU29:HN	:LYS26:O
12	:TYR12:HN	:VAL8:O	37	:TYR30:HN	:LYS26:O
13	:THR13:HN	:TYR9:O	38	:TYR30:HN	:LYS27:O
14	:THR13:HN	:ASP10:O	39	:LEU31:HN	:LYS27:O
15	:THR13:HG1	:TYR9:O	40	:LEU31:HN	:VAL28:O
16	:TRP14:HN	:ASP10:O	41	:ALA32:HN	:VAL28:O
17	:ILE15:HN	:PHE11:O	42	:ALA32:HN	:LEU29:O
18	:ALA16:HN	:TYR12:O	43	:ARG33:HN	:LEU29:O
19	:LYS17:HN	:THR13:O	44	:ARG33:HN	:TYR30:O
20	:LYS17:HN	:TRP14:O	45	:ASN34:HN	:TYR30:O
21	:LYS18:HN	:TRP14:O	46	:ASN34:HN	:LEU31:O
22	:LYS18:HN	:ILE15:O	47	:ALA35:HN	:TYR30:O
23	:VAL19:HN	:ILE15:O	48	:SER6:HB2	:VAL3:O
24	:VAL19:HN	:ALA16:O	49	:LYS17:HE2	:THR13:O
25	:ALA20:HN	:ALA16:O			

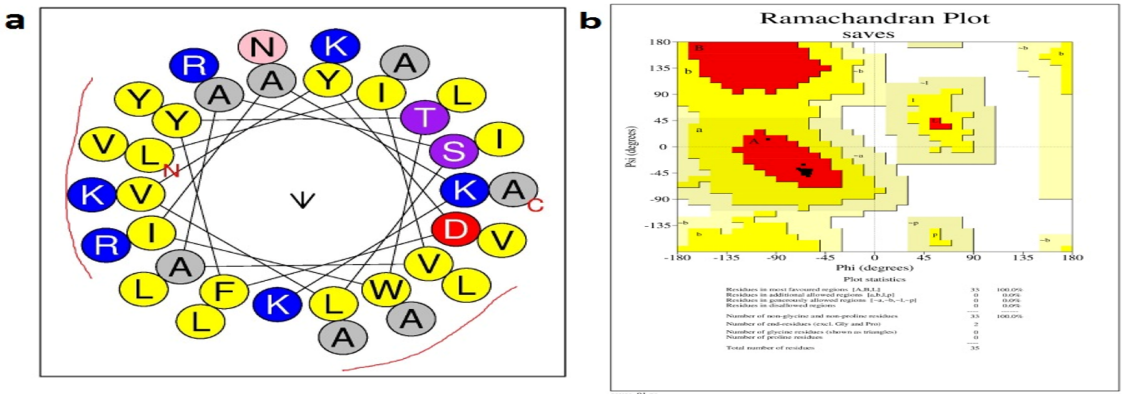


Fig. 1 Helicity assessment using HeliQuest and the quality of the 3D structure of the peptide using Ramachandran plot. (a) Helicity assessment of the peptide sequence showed that at least 6 hydrophobic residues are aligned. (b) Ramachandran plot of peptide Cliotide U1 shows that the peptide structure has favorable Phi and Psi angles and all residues are located in the most favored regions; in the helicity analysis, positively charged residues are shown in blue, negatively charged residues in pink, hydrophobic residues in yellow, sulfur-containing residues in purple, and weakly hydrophobic residues in gray. Also, hydrophobic residues distributed in one direction are marked with a red line.

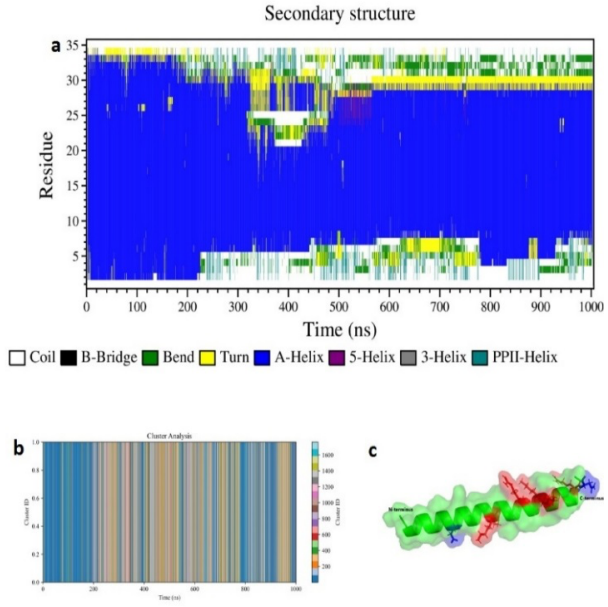


Fig. 2 Secondary structure of Cliotide U1 peptide residues, formed clusters, and peptide structure at frame 78,273 corresponding to the top cluster state during the molecular dynamic simulation. (a) Secondary structure analysis of residues showed that residues 8–20 were mostly alpha helixes, while residues 2–7 were alpha helixes for the first 220 ns but subsequently formed various secondary structures such as coils, turns, and bends. Residue 30 was alpha helixes for the first 200 ns but subsequently formed various secondary structures, most often turns; (b) Analysis of the formed clusters showed that the peptide had high structural diversity in the first 200 nanoseconds, but in the time interval 200 to 750 nanoseconds, this structural diversity decreased, but again in the continuation of the simulation process in the time interval 750 to 920, structural diversity increased, but again in the continuation until the end of the process, the peptide formed fewer clusters; (c) 3D structure of the peptide in the top cluster mode, where the backbone and molecular surface structures are shown as cartoons in green, while the side chains of positively and negatively charged residues are displayed in the Sticks style and in red and blue, respectively.

Like other plant-derived AMPs, the presence of aligned hydrophobic residues and positively charged amino acids in Cliotide U1 facilitates initial electrostatic adsorption and subsequent insertion into bacterial membranes, leading to membrane instability and permeabilization [31]. Based on HemoPI outputs, Cliotide U1 was predicted to be non-hemolytic, with a score of 0.49 (Table 2). Toxicity assessment using ToxinPred classified Cliotide U1 as non-toxic (Table 2). In addition, the dPABBs server predicted antibiofilm activity for Cliotide U1 using an SVM model based on amino-acid composition, suggesting a favorable antibiofilm potential (Table 2).

Helicity and 3D Structural Assessment

Residue distribution analysis using HeliQuest indicated a helical arrangement in which hydrophobic residues were aligned across two helical faces, a pattern that may facilitate insertion into the membrane hydrophobic core after initial electrostatic docking mediated by positively charged residues (Fig. 1a). The predicted three-dimensional structure was evaluated with PROCHECK (SAVES server), and the Ramachandran plot showed that 100% of residues fell within the most favored regions (Fig. 1b).

MD Simulation of Cliotide U1 in Aqueous Environment

Secondary-structure assignments were calculated using the DSSP algorithm and visualized as a time-evolution timeline using the Timeline plugin in VMD**.** Secondary-structure monitoring during the 1000-ns simulation showed that the central segment of the peptide (approximately residues 8–20) predominantly retained an α-helical conformation. Residues 2–7 initially formed a helix during roughly the first 220 ns but later adopted mixed secondary structures (coil, turn, PPII helix, and bend). Residue 30 also showed an early helical tendency (first ~200 ns) followed by frequent turn conformations. The terminal residues (1 and 35) remained largely in a coil state throughout the trajectory (Fig. 2a). Cluster analysis indicated notable conformational diversity in the early phase of simulation (first ~200 ns). The structural variability decreased between ~200–750 ns, increased again during ~750–920 ns, and then converged toward fewer dominant conformations toward the end of the simulation (Fig. 2b). The representative structure of the most populated cluster (top cluster) exhibited extensive intra-chain hydrogen bonding (Fig. 2c), with donor/acceptor details summarized in Table 3. In this dominant state, most residues (excluding the termini) adopted helical conformations. Several positively charged residues were positioned in a manner that likely favors interaction with negatively charged membranes, whereas the proximity of negatively charged residues on one face may reduce binding efficiency from that orientation.

Structural stability was quantified by RMSD, which showed a pronounced initial deviation (approximately 5 nm) followed by stabilization with fluctuations generally within ±1 nm (Fig. 3a). RMSF analysis further indicated higher mobility at the N- and C-termini, consistent with their coil-rich behavior, whereas the helical core exhibited lower fluctuations (Fig. 3b). Radius of gyration analysis suggested that the peptide maintained a compact overall structure, with fluctuations around ±2 nm (Fig. 3c).

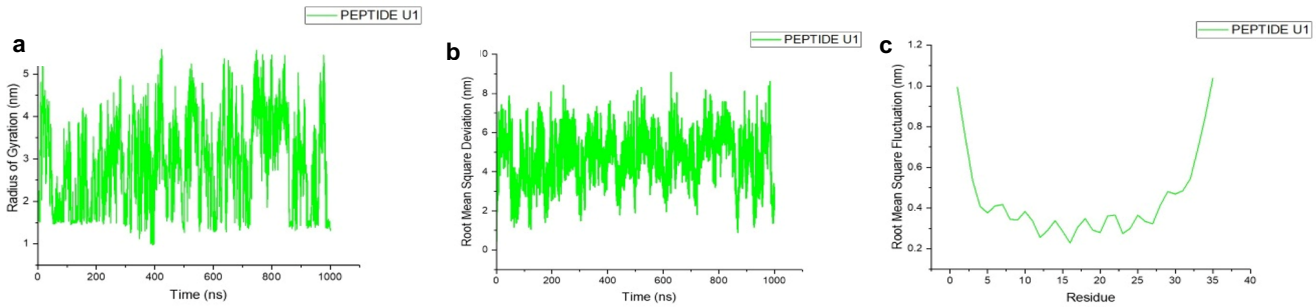


Fig. 3 Stability of the Cliotide U1 peptide during molecular dynamic simulation. (a) Structural changes of the peptide during the simulation relative to the initial state (RMSD); (b) Stability fluctuation (RMSF) of peptide residues during the simulation. (c) Changes in the radius of gyration of the peptide during the simulation (RG).

Peptide–membrane MD Simulation

Quantitative analyses demonstrated that Cliotide U1 interacted with both Gram-positive and Gram-negative membrane models, but with clearly different interaction modes. In the Gram-negative system, the peptide moved toward the lipid region and reached the membrane interface after ~20 ns, followed by more pronounced association and insertion during the subsequent frames (20–100 ns). In contrast, in the Gram-positive membrane model, penetration was minimal; only a limited and transient insertion of terminal segments into the headgroup region was observed (around ~40 ns). Overall, the peptide largely remained spread along the membrane surface throughout the simulation and did not enter the hydrophobic core.

The peptide exhibited greater conformational stability while interacting with the Gram-negative membrane and maintained its helical character over the 100-ns trajectory. In the Gram-positive system, higher structural variability was observed, particularly at the termini, which fluctuated between helix and coil (Fig. 4a, b).

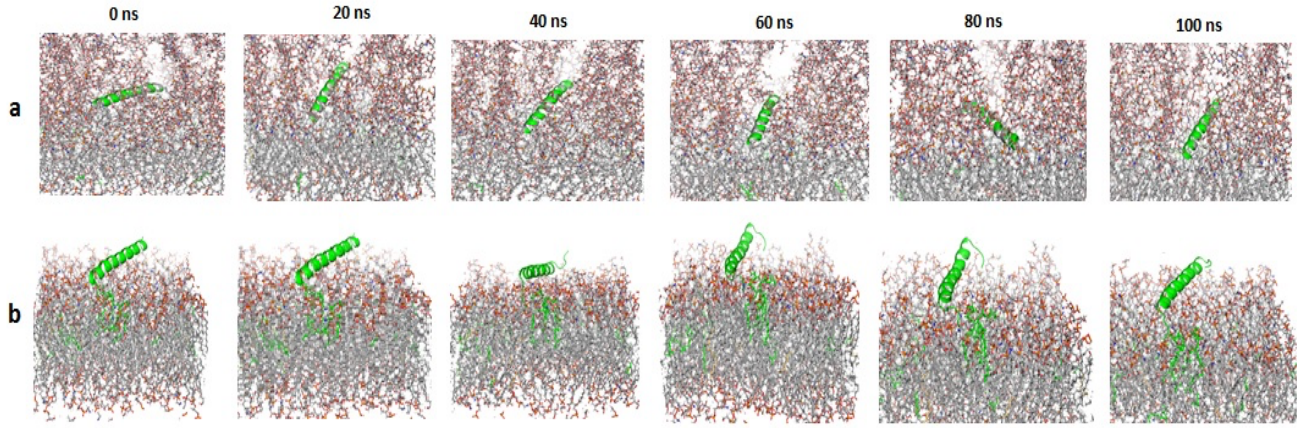


Fig. 4 Snapshots from 100-ns MD simulations of Cliotide U1 interacting with the Gram-negative (a) and Gram-positive (b) bacterial membrane models.

RMSD profiles supported earlier stabilization and lower fluctuation in the Gram-negative complex (Fig. 5a). For the Gram-positive system, more prominent backbone deviations were observed, especially between ~40–60 ns, followed by stabilization after ~60 ns. RMSF confirmed increased flexibility in the Gram-positive condition relative to the Gram-negative system (Fig. 5b). Radius of gyration analysis indicated that both peptide–membrane systems remained stable over 100 ns, although the Gram-positive simulation exhibited greater variability (Fig. 5c). Comparative RMSD and RMSF analyses further revealed that Cliotide U1 exhibits higher dynamic stability and less residue fluctuation in the Gram-negative model system. This finding supports the hypothesis that peptide–membrane binding is stronger and more specific in the Gram-negative bacteria, aligning with the higher antimicrobial activity previously reported against *Escherichia coli* and *Acinetobacter baumannii* [15]. It should be noted that these experimental data were obtained from a previously published study [15] and were used here for comparative interpretation, not generated in the present work. These observations are also consistent with the behavior of other α-helical AMPs, such as CM15 and magainin, which preferentially target negatively charged bacterial membranes while sparing mammalian cells due to charge selectivity [26, 32]. Furthermore, the formation of stable intra-chain hydrogen bonds in Cliotide U1 contributes to its helical stability, compactness, and stable interaction with membrane interfaces, enhancing its structural robustness during long-term simulation [33].

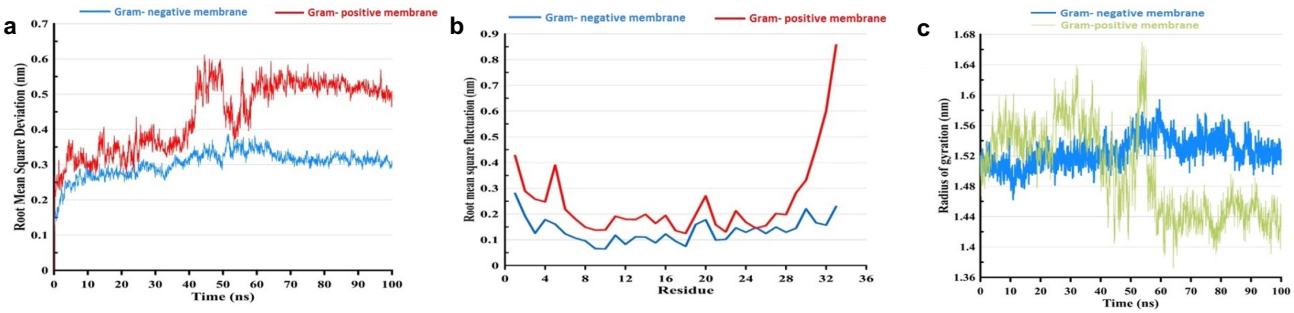


Fig. 5 Backbone RMSD (a), RMSF (b), and radius of gyration (Rg) (c) analyses of all-atom MD trajectories of Cliotide U1 in the Gram-negative and Gram-positive bacterial membrane models during 100-ns simulations.

The low hemolytic and non-toxic profile predicted by *in silico* analysis suggests that Cliotide U1 has a favorable therapeutic index. Many AMPs, with their high cationicity or hydrophobicity, suffer from cytotoxicity against mammalian cells [34]; however, the balanced distribution of hydrophobic and charged residues in Cliotide U1 minimizes non-selective membrane disruption, supporting its potential for clinical development. The predicted anti-biofilm activity further increases its biomedical importance, as biofilm-associated infections are among the most persistent and antibiotic-resistant forms of microbial colonization [35]. AMPs, which are capable of killing planktonic cells and disrupting biofilms, are of particular interest in the in the designing new anti-infective therapeutics. MD simulations show that Cliotide U1 interacts differently with the membrane of Gram-negative and Gram-positive bacteria. In the membrane of Gram-negative bacteria, the peptide penetrated the lipid region after ~20 ns. In

contrast, in the Gram-positive bacteria membrane, peptide insertion was minimal. This peptide remained predominantly on the membrane surface, which is consistent with a carpet-like mechanism in Gram-positive bacteria, were surface coverage and lipid disruption lead to membrane disruption without deep penetration [36]. These differences likely reflect the structural changes between the two membrane types. Gram-negative membranes, with an outer lipid and lipopolysaccharide layer, allow deeper peptide insertion, while Gram-positive membranes prefer surface interactions. Overall, Cliotide U1 appears to act through a pore-forming mechanism in Gram-negative bacteria and a carpet-like mechanism in Gram-positive bacteria.

Collectively, these computational observations suggest that Cliotide U1 is a highly stable and selective AMP with strong affinity for Gram-negative bacterial membranes. The integration of bioinformatics tools, structure prediction algorithms, and MD simulations provided a comprehensive understanding of its molecular behavior and demonstrated the power of *in silico* strategies for preclinical peptide evaluation. Future experimental validations, including peptide-lipid binding assays and atomic force microscopy, are necessary to confirm the predicted penetration and disruption mechanisms under physiological conditions [37].

While the present study provides a detailed in silico characterization of Cliotide U1, it is important to acknowledge that all findings are computational predictions and have not been experimentally validated in this work. The ToxinPred, HemoPI, and dPABBs predictions are based on sequence-derived features and machine-learning models, and MD simulations, although informative, are limited by force-field accuracy and timescale. The membrane models used here are simplified representations of complex bacterial membranes and do not fully capture the contributions of lipopolysaccharides, membrane proteins, or environmental factors. Future experimental studies—including antimicrobial susceptibility assays, hemolysis assays, peptide–lipid binding experiments, and microscopy—are required to confirm the predicted selectivity and membrane-disruption mechanisms under physiological conditions.

CONCLUSION

In conclusion, this study elucidates the molecular basis of antimicrobial activity of Cliotide U1 using combined bioinformatics and MD approaches. This peptide exhibits a stable α-helical structure, non-toxic and non-hemolytic properties, and strong selectivity toward Gram-negative membranes. Its capacity to penetrate LPS-rich regions and induce membrane disruption highlights its potential as a natural alternative to conventional antibiotics. The integration of bioinformatics, structure prediction, and MD simulations offers an efficient *in silico* pathway to screen and prioritize next-generation AMPs with optimal stability, selectivity, and therapeutic potential prior to experimental validation. Further *in vitro* and *in vivo* analyses are necessary to investigate the pharmacological application of Cliotide U1 in clinical and pharmaceutical contexts.

Consent for Publication

Not Applicable.

Data Availability Statement

The data that support the findings of this study are available on request from the corresponding author.

Conflict of Interests

The authors have not declared any conflict of interests.

Funding

This work was financially supported by a research grant from Deputy of research, School of Medicine, Shahid Beheshti University of Medical Sciences, Iran [Grant No. 43017422]. The funding agency has no role in the design of the project, work execution, analysis, interpretation of the data, and manuscript writing or submission.

Authors' contributions

MG: conceptualization, funding acquisition, methodology, project administration, resources, supervision, validation, writing–original draft, writing–review and editing.: MNT: data curation, formal analysis, methodology, writing original draft, writing–review and editing. GHE: data curation, formal analysis, methodology, writing original draft, writing–review and editing, investigation. AH: formal analysis, investigation, methodology, project administration.

Acknowledgments

No applicable.

REFERENCES

1. Zhang R., Xu L., Dong C. Antimicrobial peptides: an overview of their structure, function and mechanism of action. Protein and Peptide Letters. 2022;29(8):641-650.
2. Tanhaeian A., Sekhavati M.H., Moghaddam M. Antimicrobial activity of some plant essential oils and an antimicrobial-peptide against some clinically isolated pathogens. Chemical and Biological Technologies in Agriculture. 2020;7(1):13.
3. Ibrahim T.K., Khalaf W.A., Ali A.A. The Inhibitory effect of alcoholic extraction of *Pimpinella anisum* against *Candida albicans* isolated from gingivitis. Journal of Medicinal plants and By-products. 2025;14(1):93-97.
4. Najafi-Olya Z., Shakib P., Sepahdar A., Hasanvand M.H., Mousavi Z., Sarvi P., Mirzania F. Antimicrobial effect of *Pinus longifolia* Roxb. ex. Lamb. and *Pinus eldarica* Medw. fruits hydroalcoholic extract against *Candida albicans* and *Enterococcus faecalis*. Journal of Medicinal Plants and By-Products. 2026;15(3):347.
5. Nsaif R. Comparative study between *Aloe vera* extract mouth rinse and chlorhexidine mouth rinse in preventing biofilm growth on titanium dental implants. Journal of Medicinal plants and By-products. 2026;6:684-689.
6. Afkar S., Shokoohizadeh L. Antimicrobial properties and essential oil profile of *Ziziphora clinopodioides* Lam. from three regions of Lorestan Province. Journal of Medicinal plants and By-products. 2026;15(3):394-401.
7. Mahlapuu M., Håkansson J., Ringstad L., Björn C. Antimicrobial peptides: an emerging category of therapeutic agents. Frontiers in Cellular and Infection Microbiology. 2016;6:194.
8. Hancock R.E., Sahl H-G. Antimicrobial and host-defense peptides as new anti-infective therapeutic strategies. Nature Biotechnology. 2006; 24(12):1551-1557.
9. Aronica P.G., Reid L.M., Desai N., Li J., Fox S.J., Yadahalli S., Essex J.W., Verma C.S. Computational methods and tools in antimicrobial peptide research. Journal of Chemical Information and Modeling. 2021; 61(7):3172-3196.
10. Catalina-Hernandez E., Aguilella-Arzo M., Peralvarez-Marin A., Lopez-Martin M. Computational insights into membrane disruption by cell-penetrating peptides. Journal of Chemical Information and Modeling. 2025; 65(3):1549-1559.
11. Pokhrel R., Shakya R., Baral P., Chapagain P. Molecular modeling and simulation of the peptidoglycan layer of Gram-positive bacteria *Staphylococcus aureus*. Journal of Chemical Information and Modeling. 2022; 62(20):4955-4962.
12. Maleš M., Zoranić L. Simulation study of the effect of antimicrobial peptide associations on the mechanism of action with bacterial and eukaryotic membranes. Membranes. 2022;12(9):891.

13. Sani M-A., Separovic F. How membrane-active peptides get into lipid membranes. Accounts of Chemical Research. 2016; 49(6):1130-1138.
14. Rossetti P., Trollmann M.F., Wichmann C., Gutsmann T., Eggeling C., Böckmann R.A. From membrane composition to antimicrobial strategies: experimental and computational approaches to AMP design and selectivity. Small. 2025;22(16):e2411476.
15. Taheri M.N., Seyedjavadi S.S., Goudarzi M., Ebrahimipour G., Hashemi A. Cliotide U1, a Novel Antimicrobial Peptide Isolated From *Urtica dioica* Leaves. Bioinformatics and Biology Insights. 2025; 19:11779322251315291.
16. Chaudhary K., Kumar R., Singh S., Tuknait A., Gautam A., Mathur D., Anand P., Varshney G.C., Raghava G.P. A web server and mobile app for computing hemolytic potency of peptides. Scientific Reports. 2016;6(1):22843.
17. Gupta S., Kapoor P., Chaudhary K., Gautam A., Kumar R., Raghava G.P. Peptide toxicity prediction. Methods in Molecular Biology. 2014;143-157.
18. Hasannejad-Asl B., Heydari S., Azod F., Pooresmaeil F., Esmaeili A., Bolhassani A. Peptide-membrane docking and molecular dynamic simulation of *in silico* detected antimicrobial peptides from *Portulaca oleracea*'s transcriptome. Probiotics and Antimicrobial Proteins. 2024;16(5):1501-1515.
19. Sharma A., Gupta P., Kumar R., Bhardwaj A. dPABBs: a novel in silico approach for predicting and designing anti-biofilm peptides. Scientific Reports. 2016;6(1):21839.
20. Gautier R., Douguet D., Antonny B., Drin G. HELIQUEST: a web server to screen sequences with specific α-helical properties. Bioinformatics. 2008; 24(18):2101-2102.
21. Abraham M., Alekseenko A., Bergh C., Blau C., Briand E., Doijade M., Fleischmann S., Gapsys V., Garg G., Gorelov S., Gouaillardet G. GROMACS 2023.2 Manual; Zenodo. CERN European Organization for Nuclear Research: Geneve, Switzerland. 2023.
22. Huang J., Rauscher S., Nawrocki G., Ran T., Feig M., de Groot BL, Grubmüller H, MacKerell AD. CHARMM36: An improved force field for folded and intrinsically disordered proteins. Biophysical Journal. 2017;112(3):175a-176a.
23. Hess B., Bekker H., Berendsen H.J., Fraaije J.G. LINCS: A linear constraint solver for molecular simulations. Journal of Computational Chemistry. 1997;18(12):1463-1472.
24. Wu E.L., Cheng X., Jo S., Rui H., Song K.C., Dávila-Contreras E.M., Qi Y., Lee J., Monje-Galvan V., Venable R.M., Klauda J.B. CHARMM-GUI membrane builder toward realistic biological membrane simulations. Wiley Online Library 2014.
25. Epand R.M., Rotem S., Mor A., Berno B., Epand R.F. Bacterial membranes as predictors of antimicrobial potency. Journal of the American Chemical Society. 2008;130(43):14346-14352.
26. Zaeifi D., Najafi A., Mirnejad R. Molecular dynamics simulation of antimicrobial peptide CM15 in *Staphylococcus aureus* and *Escherichia coli* model bilayer lipid. Iranian Journal of Biotechnology. 2023;21(2):e3344.
27. Allen W.J., Lemkul J.A., Bevan D.R. GridMAT-MD: a grid-based membrane analysis tool for use with molecular dynamics. Journal of Computational Chemistry. 2009;30(12):1952-1958.
28. Fantner G.E., Barbero R.J., Gray DS, Belcher AM. Kinetics of antimicrobial peptide activity measured on individual bacterial cells using high-speed atomic force microscopy. Nature Nanotechnology. 2010;5(4):280-285.
29. Abraham MJ., Murtola T., Schulz R., Páll S., Smith J.C., Hess B., Lindahl E. GROMACS: High-performance molecular simulations through multi-level parallelism from laptops to supercomputers. 2015; SoftwareX 1:19-25.
30. Humphrey W., Dalke A., Schulten K. VMD: visual molecular dynamics. Journal of Molecular Graphics and Modelling. 1996;14(1):33-38.
31. Mookherjee N., Anderson MA, Haagsman HP, Davidson DJ. Antimicrobial host defence peptides: functions and clinical potential. Nature Reviews Drug Discovery. 2020;19(5):311-332.
32. Saiba R., Debnath A., Vemparala S. The role of negatively charged groups in antimicrobial cationic peptide mimics: Insights into membrane interactions. Journal of Physical Chemistry B. 2025;129(28):7134-7145.
33. Niazi S.K. Protein catalysis through structural dynamics: a comprehensive analysis of energy conversion in enzymatic systems and its computational limitations. Pharmaceutical. 2025;18(7):951.
34. Kurnaz LB., Luo Y., Yang X., Alabresm A., Leighton R., Kumar R., Hwang J., Decho AW., Nagarkatti P., Nagarkatti M., Tang C. Facial amphiphilicity index correlating chemical structures with antimicrobial efficacy. Bioactive Materials. 2023;20:519-527.
35. Miquel S., Lagrafeuille R., Souweine B., Forestier C. Anti-biofilm activity as a health issue. Frontiers in Microbiology. 2016;7:592.
36. Shai Y. Mode of action of membrane active antimicrobial peptides. Biopolymers. 2002; 66(4):236-48.
37. Morandat S., Azouzi S., Beauvais E., Mastouri A., El Kirat K. Atomic force microscopy of model lipid membranes. Analytical and Bioanalytical Chemistry. 2013:405(5):1445-1461.